Food & Function

ROYAL SOCIETY OF CHEMISTRY

PAPER

View Article Online
View Journal | View Issue

Cite this: *Food Funct.*, 2025, **16**, 71

Microencapsulation of broccoli sulforaphane using whey and pea protein: *in vitro* dynamic gastrointestinal digestion and intestinal absorption by Caco-2-HT29-MTX-E12 cells

Ali Ali Redha, *[a,b] Luciana Torquati, [a] John R. Bows, [c] Michael J. Gidley [b] and Daniel Cozzolino [b]

Sulforaphane, an organosulfur phytochemical, has been demonstrated to have significant anticancer potential in both *in vitro* and *in vivo* studies, exhibiting mechanisms of action that include inducing apoptosis, inhibiting cell proliferation, and modulating key signalling pathways involved in cancer development. However, its instability presents a major obstacle to its clinical application due to its limited bioavailability. This study aimed to improve the stability and thus the bioavailability of sulforaphane from broccoli by microencapsulation with whey (BW) and pea protein (BP) by freeze-drying. BW and BP were characterised by particle size measurement, colour, infrared spectroscopy, scanning electron microscopy, thermogravimetry, and differential scanning calorimetry. Dynamic *in vitro* gastrointestinal digestion was performed to measure sulforaphane bioaccessibility, in BP, BW and dried broccoli. A Caco-2-HT29-MTX-E12 intestinal absorption model was used to measure sulforaphane bioavailability. The *in vitro* dynamic gastrointestinal digestion revealed that sulforaphane bioaccessibility of BW was significantly higher (67.7 ± 1.2%) than BP (19.0 ± 2.2%) and dried broccoli (19.6 ± 10.4%) ($p < 0.01$). In addition, sulforaphane bioavailability of BW was also significantly greater (54.4 ± 4.0%) in comparison to BP (9.6 ± 1.2%) and dried broccoli (15.8 ± 2.2%) ($p < 0.01$). Microencapsulation of broccoli sulforaphane with whey protein significantly improved its *in vitro* bioaccessibility and bioavailability. This suggests that whey protein isolate could be a promising wall material to protect and stabilise sulforaphane for enhanced bioactivity and applications (such as nutraceutical formulations).

Received 19th July 2024,
Accepted 5th October 2024

DOI: 10.1039/d4fo03446e

rsc.li/food-function

1. Introduction

Broccoli, a cruciferous vegetable, is rich in bioactive compounds with health-promoting benefits. One of the most abundant phytochemical groups in broccoli is the glucosinolates.[1,2] Glucoraphanin ($C_{12}H_{23}NO_{10}S_3$), 1-*S*-[(1*E*)-5-(methylsulfinyl)-*N*-(sulfonatooxy)pentanimidoyl]-1-thio-β-D-glucopyranose, is one of the key glucosinolates in broccoli and its concentration ranges between 0.005 and 1.13 μmol g^{-1} of fresh weight.[3] Glucoraphanin can be hydrolysed into an organosulfur compound called sulforaphane. Sulforaphane ($C_6H_{11}NOS_2$), 1-isothiocyanato-4-(methanesulfinyl)butane, is an isothiocyanate that has been referred to as "green chemoprevention" due to its wide range of anticancer activities and availability across commonly consumed cruciferous vegetables.[4] It is capable of inhibiting cancer cell proliferation, causing apoptosis, and stopping the cell cycle.[5] In terms of mechanism, sulforaphane directly modulates histone deacetylases which are involved in chromatin remodelling, gene expression, and Nrf2 antioxidant signalling.[5] For instance, the weekly consumption of 492 μmol glucoraphanin (sulforaphane precursor)-rich broccoli soup for 12 months, significantly enhanced the downregulation of genes for reactive oxygen species and xenobiotic metabolism in the prostate tissue isolated from male patients on active surveillance.[6] The study also observed a negative correlation between the consumption of *S*-methyl cysteine sulfoxide (a sulphur-containing bioactive compound) through cruciferous vegetable intake and an increase in WHO (a contemporary prostate cancer grading system).[6] However, there are contrasting results in sulforaphane effects in clinical trials which could potentially be due to its low bioavailability.[7,8]

The formation of sulforaphane from glucoraphanin hydrolysis is achieved by the enzyme myrosinase (E.C. 3.2.3.147) and is a critical factor in determining sulforaphane bioavailability,

[a]*The Department of Public Health and Sport Sciences, University of Exeter Medical School, Faculty of Health and Life Sciences, University of Exeter, Exeter, EX1 2LU, UK. E-mail: aa1249@exeter.ac.uk, l.torquati@exeter.ac.uk*
[b]*Centre for Nutrition and Food Sciences, Queensland Alliance for Agriculture and Food Innovation (QAAFI), The University of Queensland, Brisbane, QLD 4072, Australia. E-mail: m.gidley@uq.edu.au, d.cozzolino@uq.edu.au*
[c]*PepsiCo R&D, Leicester, LE4 1ET, UK. E-mail: john.bows@pepsico.com*

particularly as it is influenced by pH (Fig. 1).[9] Glucoraphanin can hydrolyse into sulforaphane through Lossen-type rearrangement at pH 6–7, while more acidic conditions (pH 2–5) and the presence of nitrile-specifier protein (NSP) can lead to the formation of sulforaphane nitrile[10] which is biologically inactive.[11] In fact, the presence of epithiospecifier protein (ESP) and iron(II) ions can also favour the formation of sulforaphane nitrile.[12] Additionally, under basic conditions and the presence of thiocyanate-forming protein (TFP), sulforaphane thiocyanate can be formed which is biologically inactive as well.[13] Thus, controlling pH during myrosinase hydrolysis plays an important role in sulforaphane bioavailability. Myrosinase, as the key enzyme involved in converting glucoraphanin to sulforaphane, is active in the temperature range of 20–70 °C.[14] The difference in thermolability of myrosinase and ESP can be used as an advantage to inactivate ESP and enhance sulforaphane formation. It has been reported that mild heating (~60 °C) of broccoli for a short duration (~10 min) can selectively inactivate ESP while retaining the activity of myrosinase, thus enhancing the formation of sulforaphane.[15,16]

Like most alkyl isothiocyanates, sulforaphane is a lipophilic molecule,[17] and unlike its hydrophilic precursor, it has poor water solubility and stability.[18] Sulforaphane's poor stability is significantly affected by pH, temperature, light, and oxygen.[19] The reason behind this lies in the presence of an active electrophilic carbon atom in the isothiocyanate group of sulforaphane which makes this compound readily and reversibly convert to thiols yielding pH-sensitive dithiocarbamates under physiological conditions.[20] Dithiocarbamates then react with amines to form thiourea. Since sulforaphane is affected by pH, its stability through the digestion process remains a challenge as the human digestive system's pH ranges from 1.5 to 7.[21] Thus, sulforaphane needs to be protected against those influential factors in industrial food and drink processes or final preparation for consumption at-home/away-from-home as well as in the human digestive tract to ensure an appropriate bioavailability and realise its bioactive potential in the cells.

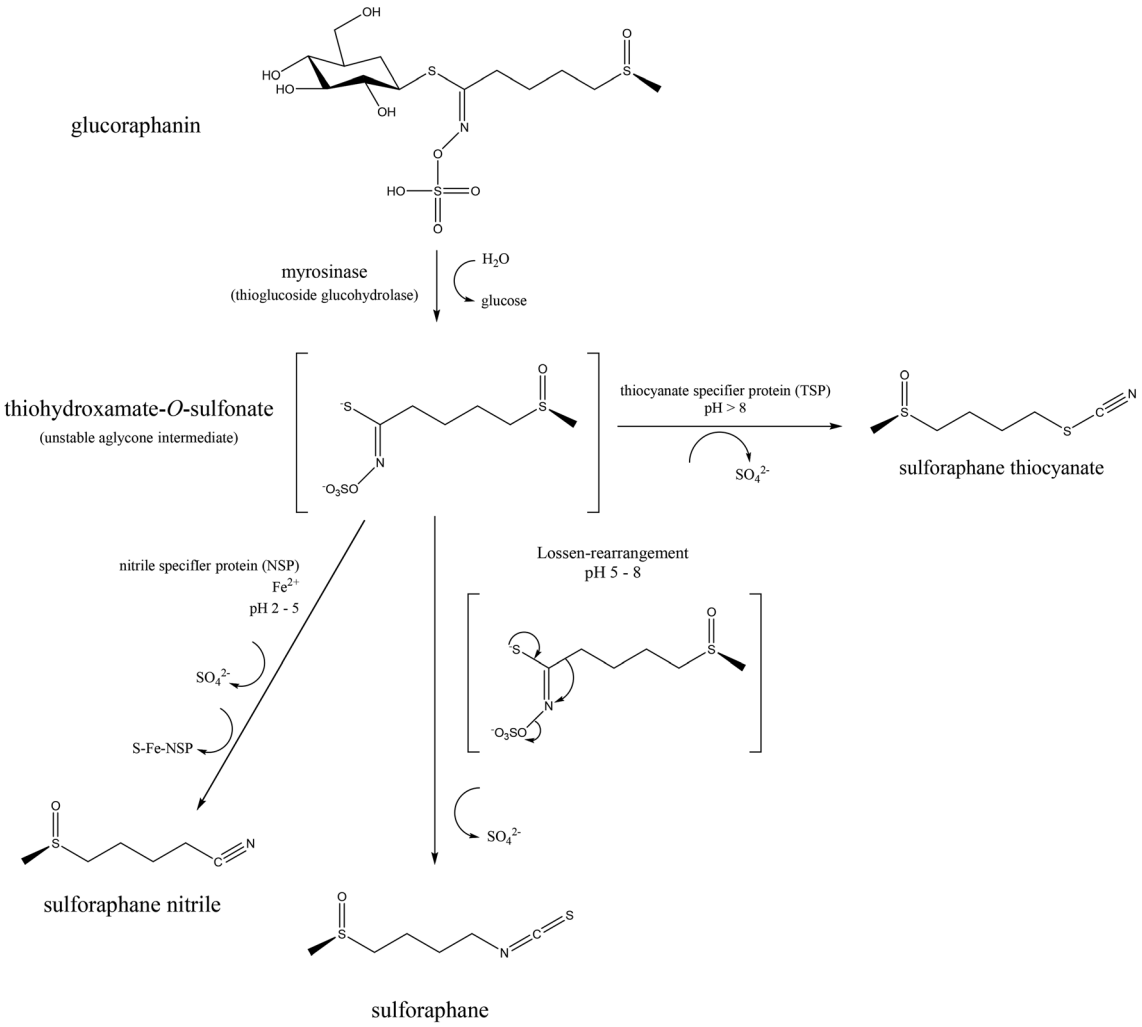

Fig. 1 Transformation of glucoraphanin into sulforaphane, sulforaphane nitrile, and sulforaphane thiocyanate under different conditions (created using ChemDraw Professional 20.0).

Encapsulation is one of the common methods that can be used to protect unstable and labile phytochemicals.[22] Proteins are a common wall material for encapsulation purposes. The surface of protein molecules contains various functional groups that facilitate effective interaction with different bioactive compounds,[23] including both hydrophilic and hydrophobic compounds, for efficient encapsulation.[24]

Among the different types of proteins, whey proteins are specifically useful for encapsulating food-bioactive compounds due to their surface activity, amphipathic structure, and high nutritional value.[24,25] Whey protein has been shown to be an effective wall material in stabilising curcumin,[26] mandarin flavonoids,[27] β-carotene,[28] and propolis extract.[29] Compared to plant proteins that have a large globular nature, whey protein is easier to work with due to its solubility over a wide pH range, small size, and flexibility.[30] Yet, the demand for plant-sourced proteins as an alternative has increased recently among consumers due to dietary restrictions and sustainability concerns.[31] Plant proteins are considered a sustainable source of proteins with lower allergenicity compared to animal-based proteins.[32] Food industries favour plant proteins due to their high abundance and low cost.[30] Among plant proteins, pea protein globulins have all the required functional characteristics that are needed for efficient incorporation into microencapsulation systems as a good wall material.[33] A wide range of phytochemicals including hydrophobic compounds such as curcumin,[34] and beta-carotene[35] have been successfully encapsulated with pea protein (as a co-wall material), resulting in increased stability. Nevertheless, encapsulation of sulforaphane using proteins has not been investigated yet.

This study aimed to investigate and compare the effect of microencapsulating broccoli sulforaphane extract with whey and pea protein on sulforaphane bioaccessibility (by *in vitro* dynamic gastrointestinal digestion) and bioavailability (using a Caco-2-HT29-MTX-E12 intestinal absorption model).

2. Materials and methods

2.1. Materials and reagents

Fresh Calabrese broccoli grown by Barden Farms Inglewood (Inglewood, Queensland, Australia) harvested in August 2023 (winter season) were used in this study. Whey protein isolate containing 90 g of protein/100 g, 0.3 g of total fat/100 g (containing saturated fat only), and 2.5 g of carbohydrates/100 g (containing sugars only) was purchased from Myprotein™ (Northwich, United Kingdom). Pea protein isolate containing 80 g of protein/100 g, 5.5 g of total fat/100 g (1.0 g of saturated fat/100 g), and 2.6 g of carbohydrates/100 g (1.0 g of sugars/100 g) was also purchased from Myprotein™ (Northwich, United Kingdom). PBS (phosphate-buffered saline) tablets were purchased from Invitrogen™ – Thermo Fisher Scientific (Carlsbad, USA) and prepared according to the manufacturer instructions (one tablet dissolved in 100 mL of Milli-Q® water at room temperature to give 10 mM phosphate, 150 mM sodium chloride, pH 7.4). Enzymes, pancreatin, and bile used for *in vitro* digestion were purchased from Sigma-Aldrich, USA. All chemicals and reagents used were of analytical grade and purchased from Merck, Germany (unless specified).

2.2. Extraction of sulforaphane

The fresh broccoli samples were washed three times using Milli-Q® water thoroughly to remove any foreign particles present in the florets. Broccoli heads were separated and immersed in a 57 °C water bath for 13 min to inactivate ESP which favours the conversion of glucoraphanin to undesirable epithionitrile products.[36,37] The broccoli florets were removed (250 g) and blended with 80 mL of PBS solution using a commercial blender until a homogenised mixture was formed. The pH of the mixture was continuously checked with a pH probe to ensure it was ~6.5–7 which favours the formation of sulforaphane. Following a previously reported extraction method,[38] with some modifications, the mixture was placed in beakers covered with aluminium foil and incubated in an ultrasonic bath (500 TD, SONICLEAN™, Australia) for 60 min at 35 °C and 100 W. The mixture was extracted twice with 300 mL of dichloromethane. The extract was dried over 20 g of sodium sulphate anhydrous powder (ChemSupply, Gillman, Australia). The sulforaphane content of the extract was analysed as described in Section 2.4. For each microencapsulation process, a volume of 55 mL of extract (containing 4.96 ± 0.39 mg of sulforaphane) was evaporated under reduced pressure at 35 °C using a vacuum concentrator (SpeedVac SPD140DDA, Thermo Fisher Scientific, USA). Each dry extract was reconstituted in 10 mL of ethanol (≥98%) to be used for microencapsulation.

2.3. Microencapsulation of sulforaphane

Broccoli sulforaphane was encapsulated with whey protein or pea protein to produce the two products BW, and BP, respectively. The whey protein solution was prepared by dissolving 10 g of whey protein in 100 mL of Milli-Q® water. The solution was allowed to stir for 2 hours at 700 rpm at room temperature. The pea protein solution was prepared by dissolving 3 g of pea protein in 100 mL of water and allowed to stir for 2 hours at 700 rpm at 70 °C. The protein concentration was selected based on the encapsulation efficiency determined in preliminary experiments in which broccoli extract was encapsulated with 2–10 g/100 mL protein wall material (data not shown). Broccoli ethanol extracts (10 mL each) were then added to the two solutions and allowed to stir for 2 hours at 700 rpm at room temperature. The solutions were then mixed using a homogeniser (T25 digital ULTRA-TURRAX®, IKA® – Thermo Fisher Scientific, USA) at 8000 rpm for 2 min to ensure complete homogenisation. The solutions were then stored at −18 °C for 48 hours to freeze the samples. The samples were dried using a freeze-dryer (Benchtop K, VirTis, USA) at −35 °C and 1000 μBar until reaching a constant mass. Finally, the dried samples were finely powdered using a mortar and pestle and then sieved through a 355 μm (45 US Mesh) sieve (Glenammer Engineering Ltd, UK). The encapsulation yield (EY) was calculated according to eqn (1). The products

were stored in sterile plastic sealed containers at −18 °C in the dark until use.

$$\mathrm{EY}(\%) = \frac{\text{mass of final dried encapsulated product}}{\text{mass of wall material} + \text{dry extract used}} \times 100 \quad (1)$$

2.4. Quantification of sulforaphane

The sulforaphane content of the crude broccoli extract and microencapsulated samples was determined using liquid chromatography-mass spectrometry (LC-MS). For the microencapsulated samples, 0.3 g of each sample was mixed with 3 mL of dichloromethane by vortexing and incubated in an ultrasonic water bath for 30 min at 30 °C and 100 W. Then, samples were vortexed and shaken using a reciprocating shaker (SSL2, Stuart, UK) for 10 min at a rate of 200 strokes per minute. The samples were then centrifuged (Centrifuge 5810 R, Eppendorf, Germany) at 3000 rpm, and 15 °C for 10 min. A volume of 1 mL of the organic layer was collected and evaporated under reduced pressure at 35 °C using a vacuum concentrator. For the crude extract, 0.1 mL of the extract was evaporated. The residue was dissolved in 0.5 mL acetonitrile (containing 1% formic acid), filtered through a nylon syringe filter (13 mm × 0.2 μm) and subjected to LC-MS analysis according to the method we developed earlier.[39] The determined sulforaphane content was then used to calculate the encapsulation efficiency (EE) according to eqn (2).

$$\mathrm{EE}(\%) = \frac{\text{amount of microencapsulated sulforaphane}}{\text{amount of sulforaphane used for microencapsulation}} \times 100 \quad (2)$$

2.5. Characterisation of microencapsulated samples

2.5.1. Particle size measurement. The particle size measurement was done using a laser diffraction and dynamic image analyser (SYNC, Microtrac, USA). The refractive index of 1.48 and 1.45 were used for analysing BW and BP samples, respectively.

2.5.2. Water activity, colour measurement and appearance. Water activity was measured using a water activity meter (LabTouch-aw, Novasina, Switzerland). The colour space variables, L^* (brightness), a^* (red-green), and b^* (blue-yellow), were measured using a colourimeter (FRU WR10, ShenZhen Wave Optoelectronics Technology, China) attached to an 8 mm adapter. The device was calibrated using a white reference plate. The data was used to calculate the chroma (C^*) and hue-angle (h) using eqn (3) and (4), respectively.

$$C^* = \sqrt{(a^*)^2 + (b^*)^2} \quad (3)$$

$$h = \tan^{-1}\left(\frac{b^*}{a^*}\right) \quad (4)$$

To evaluate the appearance, equal amounts of microencapsulated samples were added to 35 mm Petri dishes and photographed in a lightbox illuminated with two 63 LED light bars (12 000–13 000 LM).

2.5.3. Morphology. The microencapsulated samples were sprayed onto a carbon tab fixed to a 12.5 mm aluminium pin stub. Then, they were kept in a vacuum oven at 35 °C for ~15 hours, cleaned using an Evactron 25 De-Contaminator RF Plasma cleaner and coated with ~15 nm carbon using a Quorum Q150T carbon evaporative coater. Scanning electron microscopy (SEM) images were taken using a Hitachi SU3500 at 3 kV, and 1.5 kV when charging occurred on the specimen surface.

2.5.4. Infrared spectroscopy measurements. The mid-infrared (MIR) spectrum (4000–400 cm^{-1}) of the wall materials (whey and pea protein), dry broccoli extract and microencapsulated samples were obtained using a MIR spectrometer with an attenuated total reflectance (ATR) platinum diamond single reflection module (Alpha II, Bruker, USA). The resolution of the spectrum was set as 4 cm^{-1} with 24 scans. Air was considered for the reference background spectra. The data were saved using OPUS software, version 8.5, (Bruker, USA). The ATR cell was cleaned with a solution of 70% ethanol in water (v/v) and dried with laboratory Kimwipes® before measuring each sample.

2.5.5. Thermogravimetric analysis. Thermogravimetric analysis (TGA) was performed to determine the decomposition temperature (T_d) using a TGA system (STARe System TGA/DSC 3+, Mettler Toledo, USA). Under an N_2 flow of 10 cm^3 min^{-1}, the BW and BP were heated from 40 to 400 °C (at a rate of 10 °C min^{-1}).

2.5.6. Differential scanning calorimetry analysis. Differential scanning calorimetry (DSC) analysis was performed to determine the glass transition temperature (T_g) using a DSC system (STARe System DSC 3, Mettler Toledo, USA). Samples were heated under an N_2 flow of 30 cm^3 min^{-1} from 40 to 350 °C (at a rate of 10 °C min^{-1}).

2.6. *In vitro* dynamic gastrointestinal digestion: measurement of bioaccessibility

Dynamic digestion simulation was performed using the simulator of the human intestinal microbial ecosystem (SHIME) setup, a multicompartment human ecosystem simulator, which consists of five connected reactors representing the different parts of the human gastrointestinal tract.[40] The *in vitro* digestion was conducted as described previously with some modifications.[41] Only the first two reactors were used for this experiment (Fig. 2), mimicking the stomach and duodenum (referred to as 'intestine' in our study).

Microencapsulated samples (BW (2.5 g) and BP (0.5 g)) and dry broccoli powder (3.0 g) were mixed with 100 mL of simulated salivary stock solution (15.1 mM KCl, 3.7 mM KH_2PO_4, 13.6 mM $NaHCO_3$, 0.15 mM $MgCl_2(H_2O)_6$, 0.06 mM $(NH_4)_2CO_3$, 1.1 mM HCl, and 1.5 mM $CaCl_2(H_2O)_2$).[42] The mixture was stirred using a magnetic stirrer and transferred to the system's first reactor, representing the stomach. About 48 mL of simulated gastric stock solution (6.9 mM KCl, 0.9 mM KH_2PO_4, 25 mM $NaHCO_3$,

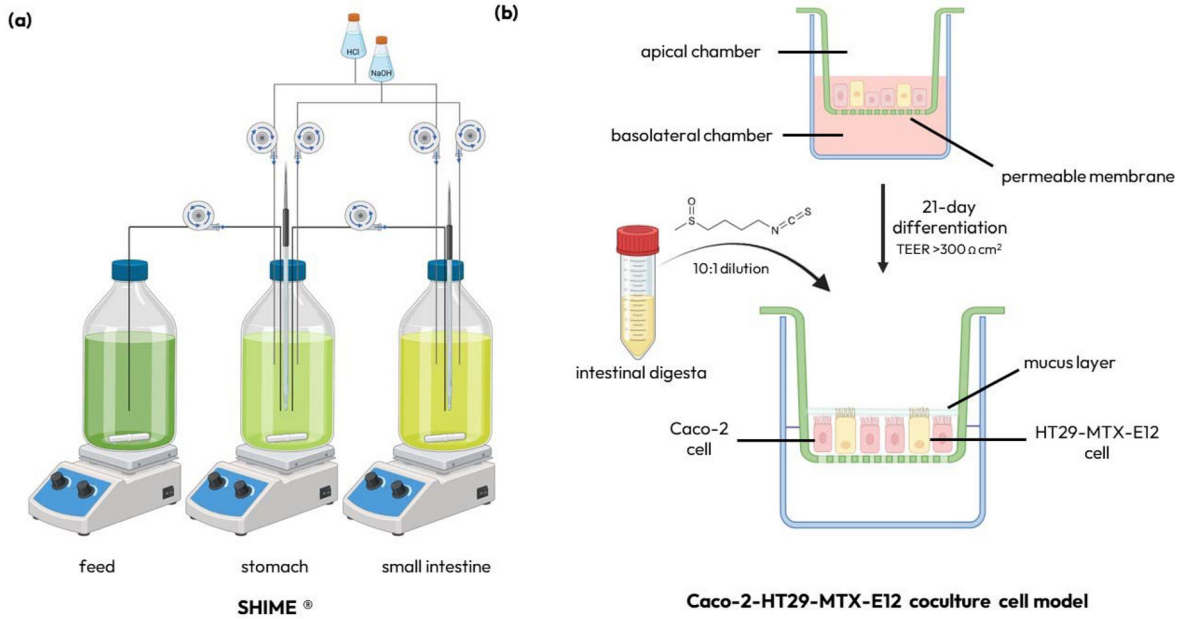

Fig. 2 Experimental setup of (a) *in vitro* dynamic gastrointestinal digestion based on SHIME ® setup, and (b) *in vitro* intestinal absorption based on Caco-2-HT29-MTX-E12 coculture cell model (created using BioRender.com).

47.2 mM NaCl, 0.12 mM $MgCl_2(H_2O)_6$, 0.5 mM $(NH_4)_2CO_3$, 15.6 mM HCl, and 0.15 mM $CaCl_2(H_2O)_2$) was added to the mixture.[42] The mixture was stirred using a magnetic stirrer and an aliquot was taken from the vessel to represent the undigested sample. Then, the pH of the remaining mixture was adjusted to 2.0, followed by the addition of 8.2 mL pepsin solution (34 070 U mL^{-1}; P6887; Sigma Aldrich, USA) to the reactor at a flow rate of 1 mL min^{-1}, to reach a final pepsin concentration of 2000 U mL^{-1} of gastric content. The gastric digestion lasted for 2 h. An aliquot was taken from the reactor at the end of the gastric digestion and its pH was adjusted to 7 with 2 M NaOH for pepsin inactivation. Two hours after the beginning of the gastric phase, the gastric content was transferred to the intestinal reactor at a flow rate of 4 mL min^{-1}. At the same time, the second reactor, representing the intestine, was fed with 45 mL of pancreatin juice containing (12.5 g L^{-1} $NaHCO_3$, 6 g L^{-1} bile (ox-bile B3883, Sigma-Aldrich, USA), and 0.9 g L^{-1} pancreatin (P3292, Sigma-Aldrich, USA)) at a flow rate of 4 mL min^{-1}. The reactors had a circulating water bath controlled at 37 °C. The pH of the two reactors was monitored using a computer-controlled program and automatically adjusted (using an integrated pH circuit (EZOTM, Atlas Scientific, USA), operated by a Raspberry Pi microprocessor (Version 1B, Raspberry Pi Foundation, UK)) to the set pH of ~2 for the gastric phase and ~7 for the intestinal phase. Intestinal digestion lasted for 2 h. Finally, the pH of the digested samples was adjusted to 11 with 2 M NaOH to inactivate the pancreatin. The samples were immediately cooled in an ice bath and subsequently frozen at −80 °C. Two replicates of each sample were subjected to dynamic *in vitro* gastrointestinal digestion.

For sulforaphane content analysis after digestion, a volume of 10 mL of each sample was extracted with an equal volume of dichloromethane. A volume of dichloromethane extract was removed and concentrated under reduced pressure, processed and the sulforaphane content was determined as described earlier (Section 2.4.). Finally, the bioaccessibility of sulforaphane was then calculated according to eqn (5).

$$\text{Bioaccessibility}(\%) = \frac{\text{amount of sulforaphane in digested sample}}{\text{amount of sulforphane in undigested sample}} \times 100 \quad (5)$$

Note: For general comparison purposes, a portion (100 g) of the fresh broccoli florets was finely crushed to release myrosinase and convert glucoraphanin to sulforaphane. After incubating at room temperature for 3 hours, the sample was air-dried in a 60 °C oven (Heratherm Oven, Thermo Fisher Scientific, USA) until reaching a constant mass. The dry broccoli was ground into a fine powder using a mortar and pestle and then sieved through a 355 μm (45 US Mesh) sieve. The sample was used as "broccoli powder" in bioaccessibility and bioavailability experiments.

2.7. *In vitro* intestinal absorption: measurement of bioavailability

2.7.1. Cell culturing. The human Caco-2 and HT29-MTX-E12 cells were purchased from the American Type Culture Collection (Manassas, VA, USA) and Sigma-Aldrich (Castle Hill, NSW, Australia), respectively. Both the cell lines were grown in Dulbecco's modified Eagle medium (DMEM) (12 mL) which was supplemented with fetal bovine serum (FBS; 10% (v/v)), non-essential amino acids (NEAA; 1×), glutamax (2 mM), streptomycin (100 μg mL^{-1}), and penicillin (100 U mL^{-1}). Cells were grown

in 75 cm^2 vented culture flasks at 37 °C and 5% CO_2. They were passaged every 2–3 days upon reaching 90% cell confluency and maintained within passages 10–25 for both cell types. Cells were counted using an automated cell counter (Countess 3, Thermo Fisher Scientific, USA) following the manufacturer protocol using 0.4% Trypan Blue solution to stain the cells. Cell suspensions were then diluted accordingly for cell passage. Cell growth was monitored and visualised using an imaging system (EVOS M5000, Thermo Fisher Scientific, USA).

To perform sub-culturing, cells were washed with 5 mL of PBS followed by the addition of 4 mL of 0.25% (v/v) trypsin–EDTA and incubation for 2–4 min to get the cells detached from the flask. A volume of 10 mL of DMEM (growth media) was then added to neutralise trypsin. Following that, the cells and growth media were centrifuged at 1500*g* for 5 min at room temperature. This was performed to pellet the cells and allow the supernatant to be replaced with fresh DMEM for cell suspension.

2.7.2. Cytotoxicity assay. The cytotoxicity of the digesta samples was measured according to the CyQUANT™ NF cell proliferation assay to determine the appropriate dilution of digesta required to produce a noncytotoxic dose–response throughout the intestinal absorption assay.[43]

To prepare the Caco-2-HT29-MTX-E12 cocultures, cells were mixed at a ratio of 9 : 1; Caco-2 cells (9000) and HT29-MTX-E12 (1000) cells with a density of 9×10^4 and 1×10^4 cells per mL, respectively. Cells were added in 100 μL growth media to each well in a Nunc™ F96 MicroWell™ black polystyrene plate and incubated at 37 °C and 5% CO_2 for 7 days.

On the experiment day, growth media was removed (~70 μL) and replaced with 100 μL HBSS and incubated for 2 h. Following 2 h of incubation, HBSS was removed and replaced with 50 μL intestinal digesta samples. Digesta samples were centrifuged at 14 000 rpm for 10 min at 10 °C and the supernatants were applied to the cells. The original intestinal digesta samples were used as well as diluted samples of ratios 2 : 1, 5 : 1, 8 : 1, 10 : 1 and 15 : 1 (diluted with HBSS). HBSS was used for the control wells. The prepared plates were incubated at 37 °C and 5% CO_2 for 2 h. After 2 h of incubation, test digesta samples were removed, and cells were washed using 100 μL of HBSS. Then, HBSS was removed and 74 μL 1× CyQUANT™ NF dye binding solution was added to each well (using a manual multichannel pipette). The plates were covered and incubated at 37 °C for 1 h. Fluorescence intensity was measured at 485 nm (excitation) and 530 nm (emission) using a multimode microplate reader (Varioskan LUX, Thermo Fisher Scientific, Singapore). The percentage of cell viability was calculated according to eqn (6).[44] The cytotoxicity assay was performed in triplicate for each digesta sample.

$$\text{Cell viability}(\%) = \frac{\text{OD}_{485-530}\ \text{treatment}}{\text{OD}_{485-530}\ \text{control}} \quad (6)$$

2.7.3. Caco-2-HT29-MTX-E12 co-culture. A co-culture of Caco-2 and HT-29-MTX-E12 cells was prepared by seeding the cells with a ratio of 9 : 1 on Costar Transwell™ plate inserts at a density of 109 000 cells per cm^2 and 12 120 cells per cm^2, respectively.[43] Cell suspension (200 μL) was added to the apical chamber and growth media (600 μL) was added to the basolateral chamber. Cells wells were incubated at 37 °C and 5% CO_2 for 21 days for cells to differentiate and form an intact monolayer. During the 21-day incubation, growth media was replaced every 2–3 days (200 μL growth media in the apical and 600 μL in the basolateral chamber).

The transepithelial electrical resistance (TEER) was measured during each media replacement using a voltohmmeter (Millicell-ERS Voltohmmeter, Merck, Germany) in an apical–basolateral direction. TEER was used to monitor cell differentiation and the formation of an intact monolayer. TEER measures the resistance and integrity of the cell monolayer and is determined based on the cellular resistance (between the apical and basolateral membrane) and the paracellular resistance (tight junctions). TEER values of >300 Ω cm^2 suggest the formation of an intact monolayer and differentiated Caco-2-HT29-MTX-E12 cells.[43]

2.7.4. Intestinal absorption assay. Prior to the experiment, TEER was measured (as described in Section 2.7.3) to ensure the integrity of the monolayer. The growth media was replaced with HBSS in the apical and basolateral chambers. The cell lines were incubated at 37 °C and 5% CO_2 for 2 h to enhance the uptake of the tested digesta in the experiment. Digested samples were diluted at a ratio of 10 : 1 using HBSS. This dilution ratio was chosen according to the results of the cytotoxicity assay that showed no change to cell viability in response to digesta samples.

The intestinal absorption experiment was performed according to a previous protocol with some modifications.[45] A volume of 200 μL of diluted intestinal digesta was added in the apical chamber (upper chamber) and 600 μL of HBSS was added in the basolateral chamber (lower chamber). Cells were incubated for a total of 4 h at 37 °C and 5% CO_2. After 2 h, the content of the basolateral chamber was collected, saved, and replaced with 600 μL of fresh HBSS. The absorption process was allowed to continue for another 2 h (total of 4 h). At the end of 4 h, the content of the basolateral chamber was collected and combined with the previous sample. The content of the apical chamber was collected and discarded. Then, a volume of 200 μL of ice-cold PBS was added to the apical chamber, and cells were scraped off and sonicated at 100 W for 20 min on ice. The cell homogenate was then centrifuged at 12 000*g* for 20 min at 4 °C. The supernatant was collected and saved. All samples were stored at −80 °C until analysis. The experiment was performed in duplicate and two additional sets of cells were also treated with growth media, and HBSS in the apical chambers for control purposes. The concentration of sulforaphane in the digesta, basolateral chamber, and cells was determined according to section 2.4. Samples were not treated and were only filtered before analysis. The bioavailability of sulforaphane was calculated according to eqn (7).[45,46]

$$\text{Bioavailablity}(\%) = \frac{\text{concentration of sulforaphane in basolateral media + cells}}{\text{concentration of sulforaphane in intestinal digesta}} \times 100 \quad (7)$$

The rate of sulforaphane movement across the membrane, also known as the apparent permeability coefficient (P_{app}), was calculated according to eqn (8).[47]

$$P_{app} = \frac{\Delta Q}{\Delta t} \times \frac{1}{A \times C_0} \quad (8)$$

where $\Delta Q/\Delta t$ is the steady-state appearance rate of sulforaphane in the basolateral chamber (μmol s^{-1}), A is the surface area of the filter (*i.e.*, 0.33 cm^2), and C_0 is the initial concentration of sulforaphane in the apical chamber (*i.e.*, digesta) (μM).

2.8. Data analysis

Experimental data were processed and presented as mean ± standard deviation of duplicate or triplicate measurements. One-way analysis of variance (ANOVA) followed by Tukey's multiple comparison tests were performed to determine significant ($p < 0.05$) differences between measurements using GraphPad Prism 10 software (Version 10.2.3, Insightful Science, LLC, USA).

3. Results and discussion

3.1. Microencapsulation

Achieving a desired intake of sulforaphane through broccoli consumption or glucoraphanin-containing supplements can be challenging. Insufficient myrosinase activity, coupled with other biochemical factors, can favour the generation of alternative glucoraphanin hydrolysis products lacking identified bioactivity. To overcome this limitation and ensure consistent delivery of sulforaphane, the present study employed a microencapsulated, sulforaphane-rich extract derived from fresh broccoli.

To enhance sulforaphane bioavailability and delivery, broccoli sulforaphane-containing extract was encapsulated using proteins as the wall material. In addition, as proteins break down in the digestive system, they release a variety of peptides that may offer additional health benefits such as antioxidant, anti-inflammatory, antidiabetic, antihyperlipidemic, antihypertensive, anticancer, and antibacterial activities.[48] Thus, encapsulating sulforaphane with proteins offers a two-fold benefit: it can not only protect the compound but also potentially enhance the overall nutraceutical value of the product.

In the current study, the EY of BW (96.9 ± 1.3%) was significantly greater than that of BP (92.0 ± 2.7%) ($p < 0.05$). Nevertheless, the EE did not differ significantly when using different proteins as wall materials ($p > 0.05$). The EY was high (+90%), yet the EE was not ideal and ranged between 50–60% (Table 1). The loss of sulforaphane in the process could potentially be due to degradation in the aqueous media.[49] Considering the nature of the wall material and the drying method selected, water was the most suitable solvent. Moreover, the EE is higher than found in a previous study in which broccoli seed sulforaphane extract was microencapsulated by gelatin/gum arabic (EE = 12.17 ± 0.10%) and gelatin/pectin (EE = 17.91 ± 1.27%) complexes.[38] Other studies that have investigated the encapsulation of broccoli sulforaphane did not report the EE.[50–52]

In terms of the microencapsulation mechanism, it is expected that sulforaphane functional groups form different interactions with various amino acids in proteins. Sulforaphane has two polar functional groups: an isothiocyanate group (–N═C═S) and a sulfoxide group (R_2-S═O). The polar groups of sulforaphane are expected to bind strongly with polypeptide C═O, C–N and N–H groups.[53] *In silico* evidence has shown the ability of sulforaphane to interact hydrophobically and simultaneously with valine, tyrosine, lysine, tryptophan, and phenylalanine;[54] as well as isoleucine, threonine and tyrosine[55] by van der Waals forces, presumably involving the alkyl region of sulforaphane. In addition, sulforaphane is capable of forming strong hydrogen bonds with glycine, valine,[56] and tyrosine.[55]

3.2. Characterisation of encapsulated materials

The encapsulated products (BW and BP) were characterised by various methods including particle size analysis, water activity, colour, visual appearance, SEM, MIR, TGA, and DSC.

The particle size analysis (Table 1) showed that the 10th percentile ($d10$) size of BW and BP particles was 43.82 and 45.43 μm, respectively. The 90th percentile ($d90$) size of BW and BP particles was 317.8 and 256.6 μm, respectively. This suggests that the majority of BW particles ranged between approximately 40 and 300 μm, while BP particles ranged between 45 and 260 μm. The mean volume diameter, $D[4,3]$, of BW and BP was 150.5 and 124.1 μm, respectively which is common for freeze-dried microencapsulated powders of plant extracts.[57,58]

In terms of water activity, BW and BP had an a_w lower than 0.3 (threshold limit) (Table 1), which suggests that the products can be regarded as stable and resilient against the impact of spoilage microorganisms and enzymes that trigger lipid oxidation.[59] With respect to colour, both samples had an L^* value >50, a negative a^* value, and a positive b^* value (Table 1), indicating that the samples were light with a tendency to a greenish and yellowish colour. For both samples, the values of h confirm that the colour falls within the blue-green region of the colour wheel. The low C^* value of both samples suggests that they were relatively desaturated. Overall, in terms of colour, both samples had a light, desaturated greenish hue. By appearance, both samples were fine green powders, with BP being slightly darker than BW due to a higher extract-to-wall material ratio in comparison to BW (Table 1). The green colour of the powders comes from the chlorophyll naturally present in the broccoli extract.

To understand the morphology of the products, the surface of BW and BP was analysed by SEM. As seen in Table 1, both BW and BP had an irregular shape which is a common characteristic of microencapsulated products formed by freeze-drying. This is due to the grinding of the dried sample which results in the formation of sheet-like particles of irregular shapes and sizes.[60] Nevertheless, the surface texture of BW and BP differed. BW had a smooth surface (Table 1), while BP had a rough, porous and wrinkled surface (Table 1). The variations seen in the morphology of freeze-dried powder are gen-

Table 1 Characteristics of microencapsulated broccoli extract with whey protein (BW) and pea protein (BP)

Microencapsulated sample		BW	BP
Sulforaphane content (mg g^{-1})		0.280 ± 0.016	0.755 ± 0.025
Encapsulation yield, EY (%)		96.9 ± 1.3[a]	92.0 ± 2.7[b]
Encapsulation efficiency, EE (%)		57.2 ± 3.3[a]	52.0 ± 1.7[a]
Particle size (μm)	Mean volume diameter, MV – d[4,3]	150.5	124.1
	Mean number diameter, MN	36.32	43.92
	Mean area diameter, MA – d[3,2]	88.55	81.96
	Standard deviation	108.9	76.91
	10^{th} percentile, $d10$	43.82	45.43
	50^{th} percentile (median diameter), $d50$	120.4	93.59
	90^{th} percentile, $d90$	317.8	256.6
Water activity, a_w		0.091 ± 0.000	0.212 ± 0.003
Colour	L^*	81.87 ± 1.38	70.10 ± 0.62
	a^*	−3.05 ± 0.18	−1.34 ± 0.20
	b^*	17.19 ± 1.44	19.09 ± 0.07
	C^*	16.92	19.14
	h (°)	−78.50	−85.98
Appearance			
Decomposition temperature, T_d (°C)		321.66	324.92
Glass transition temperature, T_g (°C)		79.88	75.35
Surface morphology		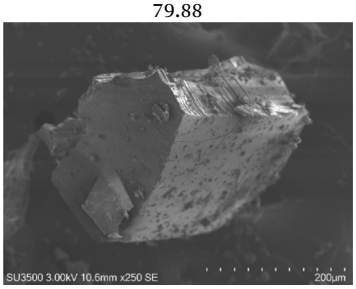	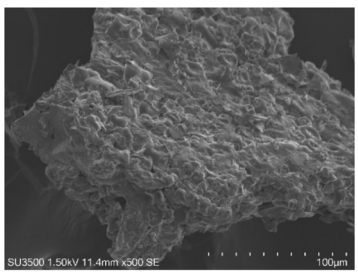

For the experiments conducted in triplicates, the values are reported as mean ± standard deviation of three trials. For EY and EE, different letters indicate that the values are significantly different ($p < 0.05$). The standard deviation of the particle size describes the width of the measured particle size distribution (not statistical error of the mean of multiple measurements). The T_d of whey protein isolate and pea protein isolate were also determined to be 309.18 and 319.85 °C, respectively.

erally due to differences in the properties of encapsulating material.[61] Microencapsulated samples prepared by freeze-drying typically have the core compound dispersed within the encapsulating material.[62] The homogeneity of the dispersion depends on the formulation and processing conditions.

The wall materials, broccoli extract, and microencapsulated products were characterised by MIR spectroscopy (Fig. 3). Whey and pea protein isolates had a similar spectrum in general with some minor differences. Both had bands at 1630 and 1515 cm^{-1} which are characteristic bands in proteins representing the peptide bonds of primary amide (–CO-NH_2) and secondary amide (–CO-NH), respectively.[63] A difference between whey and pea protein isolates was seen in the region of 3000–2800 cm^{-1}. Some bands were seen in whey protein isolate in this region which are associated with the C–H stretching vibrations of carbonyl groups of triglycerides.[63] The broccoli extract had several key bands. The sharp bands at 2915 and 2847 cm^{-1} can be associated with C–H based on the pure sulforaphane spectrum in a previous study.[64] The doublet peaks between 2200 and 2000 cm^{-1} can be correlated with the isothiocyanate group (–N═C═S) asymmetric stretching.[65] The band seen around 1740–1700 cm^{-1} can be related to the carbonyl (C═O) of an ester group from chlorophyll,[66] while that seen at 1460 can be associated with aromatic C–C stretch. The bands in the regions 1400–1300 and 800–700 cm^{-1} can be correlated with C–H, while those between 700 and 500 cm^{-1} could be linked with C–S.[64] The minor peak between 570 and 520 cm^{-1} could be associated with the deformation nodes perpendicular to –NCS plane (out-of-plane).[67] Both microencapsulated samples have a generally similar spectrum. Nevertheless, unlike BW, BP had more noticeable changes in comparison to its wall material, especially in the regions 3400–3200 and 3000–2800 cm^{-1} which could be correlated with N–H and C–H stretching, respectively. In addition, microencapsulation resulted in a stronger absorption band between 3300 and 3200 cm^{-1}, which corresponds to the stretching vibrations of –OH linked to –NH_2.[68] In BW, there were no major changes compared with a whey protein isolate spectrum other than

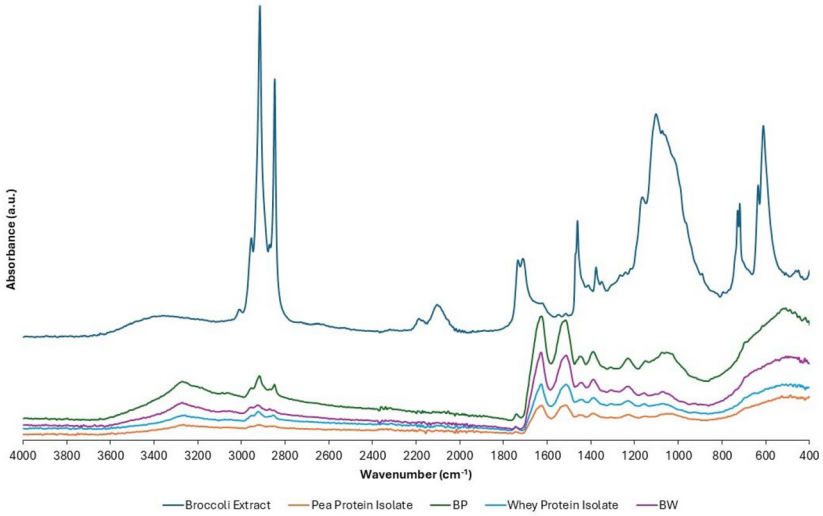

Fig. 3 Mid-infrared spectrum of broccoli extract, whey protein isolate and microencapsulated broccoli extract with whey protein (BW), pea protein isolate, and microencapsulated broccoli extract with pea protein (BP).

changes in the shape of the bands in the region between 3000 and 2800 cm^{-1}. This may be due to differences in the extract-to-wall material ratio in BW and BP. In general, the MIR analysis showed that the microencapsulated samples had a similar spectrum with respect to the wall materials. This suggests that the microencapsulation process was efficient[69] and the extract was well coated.

As a part of the characterisation experiments, the T_d and T_g of the microencapsulated were also determined. The T_d of BW and BP were close and about 320 °C (Table 1). At this temperature, the powder would start to break down chemically. The T_g of BW was about 80 °C, while that of BP was about 75 °C (Table 1). At these temperatures, the rigid powder turns softer and rubbery. These results can potentially help future industrial investigations in assessing the caking, flowability, and moisture sorption of the powder during storage. Nevertheless, it is important to highlight that sulforaphane could undergo degradation at lower temperatures due to its thermal sensitivity which requires further investigation.

3.3. Bioaccessibility

In vitro dynamic gastrointestinal digestion was used to determine differences between the bioaccessibility of sulforaphane from BW, BP, and dried broccoli. This digestion model mimicked the upper gastrointestinal tract (stomach and small intestine). The lower gastrointestinal tract (colon/large intestine) was not considered for this study because the compound of interest, sulforaphane, which has been microencapsulated is readily transported through the intestinal epithelium by passive transport.[70] The current study evaluated the use of dynamic *in vitro* digestion (SHIME setup) to determine sulforaphane bioaccessibility. Previous studies have mainly used static *in vitro* digestion for this purpose.[17,71] In this method, each phase is performed with a single set of starting conditions, such as enzyme concentration, pH, and bile salts, which do not reflect the constant biochemical changes that happen *in vivo*.[72] On the other hand, the dynamic *in vitro* digestion model allows pH regulation, food flow in different compartments, and real-time injection of digestive enzymes into various parts of the gastrointestinal tract showing a greater potential of replicating the *in vivo* digestion process.[73]

In this study, the bioaccessibility of sulforaphane from BW was significantly greater (67.7 ± 1.2%) than BP (19.0 ± 2.2%) and dried broccoli (19.6 ± 10.4%) ($p < 0.01$) as shown in Fig. 4a. In other words, a higher amount of sulforaphane was able to reach the small intestine for absorption when microencapsulated with whey protein. According to these results, whey protein isolate is a more promising wall material for sulforaphane delivery in comparison to pea protein isolate. In fact, the bioaccessibility of sulforaphane from BP and dried broccoli did not differ significantly ($p > 0.05$). The stability of sulforaphane throughout gastrointestinal digestion may be attributed to the type and strength of intermolecular interactions between sulforaphane and whey protein components (amino acids). Whey protein comprises β-lactoglobulin, α-lactalbumin, immunoglobulins, bovine serum albumin, bovine lactoferrin, and lactoperoxidase,[74] thus higher concentration of valine, leucine, and isoleucine in comparison to pea protein.[75] On the other hand, pea protein contains mainly legumin and vicilin.[76] Since sulforaphane has shown strong hydrogen bonding with valine,[56] and hydrophobic interactions with isoleucine[55] and valine,[54] this might explain the higher stability of sulforaphane observed in BW compared to BP. Thus, the differing compositions of whey and pea protein (type, amino acid sequence, and amino acid profile) are likely to influence the nature of intermolecular interactions that can form between sulforaphane and these wall materials. Further studies evaluating the amino acid composition of the microencapsulation material have great potential in increasing sul-

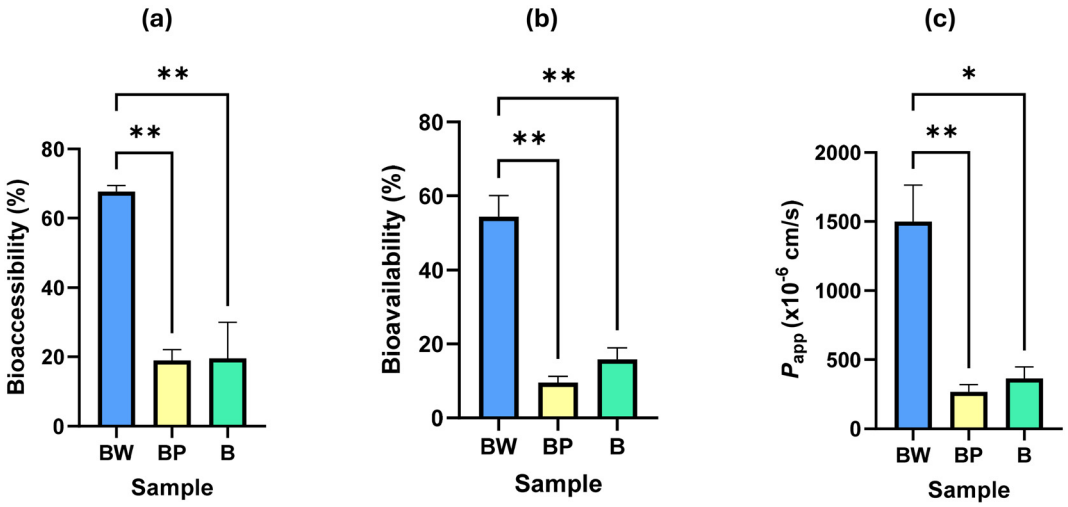

Fig. 4 Bioaccessibility (a), bioavailability (b), and apparent permeability coefficient (c) of microencapsulated broccoli extract with whey protein; BW, microencapsulated broccoli extract with pea protein; BP, and broccoli powder (B). Data presented as mean ± standard deviation, with * and ** indicating a significant difference at $p < 0.05$ and $p < 0.01$, respectively.

foraphane stability and bioaccessibility. In addition, proteins derived from other sustainable protein sources such as cereals, legumes, and oilseeds could be investigated as wall materials.

Larger microparticles are associated with a controlled release, which can be beneficial for sustained delivery of encapsulated active compounds.[77] According to the particle size analysis described earlier, BW had a larger mean volume diameter (150.5 μm) in comparison to BP (124.1 μm). This may have also positively affected the bioaccessibility of BW sulforaphane.

To date, one reported study has investigated the encapsulation of sulforaphane and performed *in vitro* gastrointestinal digestion. The study used cauliflower-derived plasma membrane vesicles to nano-encapsulate sulforaphane-containing Bimi® broccoli extract.[51] It reported that, following *in vitro* gastrointestinal digestion, the concentration of sulforaphane in the nanoencpasulated tested sample was six times higher in comparison to the free extract ($p < 0.05$). Yet, the bioaccessibility was not calculated which complicates the comparison with our results. In fact, using plasma membrane vesicles (also known as liposomes) may have some disadvantages. They have low solubility and high production cost, phospholipids may undergo oxidation or hydrolysis, and the core material is capable of leaking.[78] Thus, this may make it less applicable for large-scale production by the industrial sector compared with (whey) protein encapsulation. In addition, the use of proteins for encapsulation, such as whey, can generate bioactive peptides during digestion which can have biological benefits.[79] Peptides derived from whey protein have been reviewed and have shown promising *in vitro* antioxidant (*via* lipid peroxidation inhibition, reactive oxygen species inactivation, and free radical scavenging), anti-hypertensive (*via* angiotensin-converting enzyme inhibition), and anti-diabetic (*via* inhibition of dipeptidyl peptidase iv, α-amylase, and α-glucosidase) potential.[79]

3.4. Bioavailability

The *in vitro* bioavailability of the digested BW, BP, and dried broccoli sulforaphane was evaluated using the Caco-2-HT29-MTX-E12 intestinal absorption model. This model resembles the human small intestine better than the widely used single-cell Caco-2 model.[80] Caco-2 cells lack mucus production which acts as a physical and chemical defence layer against different food particles, enzymes, chemicals, and many host-secreted products.[81] The absence of a mucus layer facilitates the diffusion of small molecules, potentially leading to an overestimation of their permeability across the cells. In contrast, HT29-MTX-E12 are goblet cells that secrete mucins. Thus, a co-culture of Caco-2-HT29-MTX-E12 is expected to produce a cell layer closely resembling the permeability of the intestine.[81] While not investigated in this study, previous research has demonstrated that this cell model can predict intestinal permeability and categorise drugs into the biopharmaceutical classification system (BCS) based on their high or low permeability.[82]

The current study is the first to investigate the bioavailability of sulforaphane using a Caco-2-HT29-MTX-E12 cell model. The study revealed that the bioavailability of BW sulforaphane (54.4 ± 4.0%) was significantly greater than that of sulforaphane from BP (9.6 ± 1.2%) and dried broccoli (15.8 ± 2.2%) ($p < 0.01$) as shown in Fig. 4b. In addition, the P_{app} of BW sulforaphane ($1499 \times 10^{-6} \pm 265$ cm s^{-1}) was significantly greater than that of sulforaphane from BP ($266 \times 10^{-6} \pm 53$ cm s^{-1}) and dried broccoli ($272 \times 10^{-6} \pm 83$ cm s^{-1}) ($p < 0.01$) as shown in Fig. 4c. The bioavailability and P_{app} of sulforaphane from BP and dried broccoli did not differ significantly ($p > 0.05$). Based on these results, microencapsulation of broccoli

extract with whey protein enhances sulforaphane bioavailability. The physicochemical properties of the digesta of BW, including the solubility of sulforaphane in that, could potentially support improved sulforaphane intestinal uptake in comparison to BP and dried broccoli. Furthermore, the composition of the BW digesta (hydrolysed whey protein) could have also favoured the transport of sulforaphane in contrast to BP and dried broccoli. The digesta matrix composition is one of the factors that affects bioavailability.[83]

Reviewing the literature, only two studies have investigated the *in vitro* intestinal absorption (using Caco-2 cell model) of sulforaphane which was sourced from kale[46] and a broccoli seed extract.[45] The studies reported a bioavailability of 29.4 and 72.4%, respectively. The bioavailability of broccoli seed extract sulforaphane was greater than the sulforaphane from the samples of the current study. It is important to note that the previous study[45] measured sulforaphane metabolites and considered their concentration in calculating the bioavailability. The study reported that about 15% of the value was attributed to sulforaphane-glutathione and sulforaphane-cysteine. About 58% of the value was associated with sulforaphane concentration which is close to the value obtained for BW sulforaphane in the current study. It is critical to highlight that these previous studies[45,46] have considered Caco-2 cell models which lack mucus layer and may overestimate transport levels.[81] In addition, the study by Zhu *et al.* (2023)[45] did not state whether the broccoli seed extract used in their bioavailability experiment was an undigested sample or obtained from their *in vitro* digestion experiment.

Sulforaphane is passively absorbed by enterocytes (small intestinal absorptive cells) due to its lipophilicity ($\log P$ (octanol/water) = 0.72) and low molecular weight (177 g mol^{-1}).[84–86] It has been reported in some studies that upon absorption in intestinal epithelial cells, sulforaphane is rapidly conjugated with glutathione to form sulforaphane-glutathione (SNF-GSH) conjugate and then transported through the circulatory system and then metabolised by the mercapturic acid pathway (involving the liver, kidney, and small intestine).[84,87–89] The conjugation could happen without the need for catalysis, although glutathione S-transferase (GST) could potentially catalyse this reaction.[87] In low glutathione conditions, the SNF-GSH conjugate could be cleaved, resulting in free sulforaphane being circulated and transported to cells.[88] Considering that sulforaphane passively transports through the intestinal layer[70] and its metabolism partly starts at this stage,[45] future studies can consider analysing the concentration of some initial sulforaphane metabolites such as SNF-GSH. *In vivo* studies can consider further metabolites to assess bioavailability. SNF-GSH undergoes a series of enzymatic metabolic reactions to produce sulforaphane-cysteine glycine conjugate, sulforaphane-cysteine conjugate, and finally sulforaphane-*N*-acetylcysteine conjugate which is exerted in urine.[90] Measurement of these sulforaphane conjugates can help in understanding the *in vivo* bioavailability.

4. Conclusions

Broccoli sulforaphane-rich extract was microencapsulated with whey protein isolate and pea protein isolate producing products with a high EY and moderate EE. Microencapsulation of broccoli sulforaphane using whey protein was able to significantly enhance the bioaccessibility and bioavailability of sulforaphane in comparison to sulforaphane from dried broccoli and broccoli sulforaphane microencapsulated by pea protein isolate. In addition, the rate of sulforaphane movement across the membrane of Caco-2-HT29-MTX-E12 cells was significantly higher in the whey protein, compared to the pea protein microencapsulated sample. This suggests that whey protein isolate could be a promising wall material to protect and stabilise sulforaphane. Future studies could evaluate the stability of this formulation at different temperatures and humidity levels to understand the changes in sulforaphane concentration during storage. In addition, the preparation of the sulforaphane-rich broccoli extract using greener and more compatible food-grade solvents such as natural deep eutectic solvents (NADES), replacing dichloromethane, can be investigated. The composition of NADES suitable for extracting sulforaphane is yet to be investigated. Moreover, the generated peptides during the digestion of proteins can be determined and characterised. After optimising extraction, microencapsulation, and storage conditions, the *in vivo* bioavailability of sulforaphane in humans could be assessed.

Author contributions

Ali Ali Redha: conceptualization; data curation; formal analysis; investigation; methodology; software; visualization; writing – original draft; writing – review & editing; project administration. Luciana Torquati: writing – review & editing; supervision. John R. Bows: resources; writing – review & editing. Michael J. Gidley: writing – review & editing; supervision. Daniel Cozzolino: resources; writing – review & editing; supervision; project administration.

Data availability

The authors confirm that the data supporting the findings of this study are available within the article. Additional data that support the findings of this study are available from the corresponding author, AAR, upon reasonable request.

Conflicts of interest

Author John R. Bows is an employee of PepsiCo, Inc. All other authors declare no conflicts of interest.

Acknowledgements

The authors would like to thank Hung Hong, Joseph Nastasi, Bernadine Flanagan, Francis McCallum, Oladipupo Adiamo, Saleha Akter, and Jordan Poitras from The University of Queensland for their assistance in this project. The authors acknowledge the facilities, and the scientific and technical assistance, of the Microscopy Australia Facility at the Centre for Microscopy and Microanalysis (CMM), The University of Queensland. The authors acknowledge the funding made available from PepsiCo, Inc. which supported this work (*in vitro* dynamic gastrointestinal digestion and intestinal absorption experiments). The views expressed in this report are those of the authors and do not necessarily represent the position of policy of PepsiCo, Inc. Financial support for this study was also provided by the QUEX Institute, a partnership between The University of Queensland and the University of Exeter. For the purpose of open access, authors have applied a 'Creative Commons Attribution (CC BY) licence to any author accepted manuscript version arising'.

References

1 F. Langston, A. Ali Redha, G. R. Nash, J. R. Bows, L. Torquati, M. J. Gidley and D. Cozzolino, Qualitative analysis of broccoli (Brassica oleracea var. italica) glucosinolates: Investigating the use of mid-infrared spectroscopy combined with chemometrics, *J. Food Compos. Anal.*, 2023, **123**, 105532.

2 A. Ali Redha, F. Langston, G. R. Nash, J. R. Bows, L. Torquati, M. J. Gidley and D. Cozzolino, Determination of glucosinolates in broccoli (Brassica oleracea var. italica) by combining mid–infrared (MIR) spectroscopy with chemometrics, *Int. J. Food Sci. Technol.*, 2023, **58**, 5679–5688.

3 Y. Yagishita, J. W. Fahey, A. T. Dinkova-Kostova and T. W. Kensler, Broccoli or Sulforaphane: Is It the Source or Dose That Matters?, *Molecules*, 2019, **24**, 3593.

4 D. B. Nandini, R. S. Rao, B. S. Deepak and P. B. Reddy, Sulforaphane in broccoli: The green chemoprevention!! Role in cancer prevention and therapy, *J. Oral Maxillofac. Pathol.*, 2020, **24**, 405.

5 P. Jabbarzadeh Kaboli, M. Afzalipour Khoshkbejari, M. Mohammadi, A. Abiri, R. Mokhtarian, R. Vazifemand, S. Amanollahi, S. Yazdi Sani, M. Li, Y. Zhao, X. Wu, J. Shen, C. H. Cho and Z. Xiao, Targets and mechanisms of sulforaphane derivatives obtained from cruciferous plants with special focus on breast cancer - contradictory effects and future perspectives, *Biomed. Pharmacother.*, 2020, **121**, 109635.

6 M. H. Traka, A. Melchini, J. Coode-Bate, O. Al Kadhi, S. Saha, M. Defernez, P. Troncoso-Rey, H. Kibblewhite, C. M. O''Neill, F. Bernuzzi, L. Mythen, J. Hughes, P. W. Needs, J. R. Dainty, G. M. Savva, R. D. Mills, R. Y. Ball, C. S. Cooper and R. F. Mithen, Transcriptional changes in prostate of men on active surveillance after a 12-mo glucoraphanin-rich broccoli intervention-results from the Effect of Sulforaphane on prostate CAncer PrEvention (ESCAPE) randomized controlled trial, *Am. J. Clin. Nutr.*, 2019, **109**, 1133–1144.

7 J. J. Alumkal, R. Slottke, J. Schwartzman, G. Cherala, M. Munar, J. N. Graff, T. M. Beer, C. W. Ryan, D. R. Koop, A. Gibbs, L. Gao, J. F. Flamiatos, E. Tucker, R. Kleinschmidt and M. Mori, A phase II study of sulforaphane-rich broccoli sprout extracts in men with recurrent prostate cancer, *Invest. New Drugs*, 2015, **33**, 480–489.

8 L. L. Atwell, Z. Zhang, M. Mori, P. Farris, J. T. Vetto, A. M. Naik, K. Y. Oh, P. Thuillier, E. Ho and J. Shannon, Sulforaphane Bioavailability and Chemopreventive Activity in Women Scheduled for Breast Biopsy, *Cancer Prev. Res.*, 2015, **8**, 1184–1191.

9 L. Janczewski, Sulforaphane and Its Bifunctional Analogs: Synthesis and Biological Activity, *Molecules*, 2022, **27**, 1750.

10 S. Karanikolopoulou, P.-K. Revelou, M. Xagoraris, M. G. Kokotou and V. Constantinou-Kokotou, Current Methods for the Extraction and Analysis of Isothiocyanates and Indoles in Cruciferous Vegetables, *Analytica*, 2021, **2**, 93–120.

11 N. V. J. Matusheski and H. Elizabeth, Comparison of the Bioactivity of Two Glucoraphanin Hydrolysis Products Found in Broccoli, Sulforaphane and Sulforaphane Nitrile, *J. Agric. Food Chem.*, 2001, **49**, 5743–5749.

12 N. V. Matusheski, R. Swarup, J. A. Juvik, R. Mithen, M. Bennett and E. H. Jeffery, Epithiospecifier Protein from Broccoli (*Brassica oleracea* L. ssp. *italica*) Inhibits Formation of the Anticancer Agent Sulforaphane, *J. Agric. Food Chem.*, 2006, **54**, 2069–2076.

13 J. Roman, D. Gonzalez, M. Inostroza and A. Mahn, Molecular Modeling of Epithiospecifier and Nitrile-Specifier Proteins of Broccoli and Their Interaction with Aglycones, *Molecules*, 2020, **25**, 772.

14 N. Travers-Martin, F. Kuhlmann and C. Muller, Revised determination of free and complexed myrosinase activities in plant extracts, *Plant Physiol. Biochem.*, 2008, **46**, 506–516.

15 G. V. Bricker, K. M. Riedl, R. A. Ralston, K. L. Tober, T. M. Oberyszyn and S. J. Schwartz, Isothiocyanate metabolism, distribution, and interconversion in mice following consumption of thermally processed broccoli sprouts or purified sulforaphane, *Mol. Nutr. Food Res.*, 2014, **58**, 1991–2000.

16 N. V. Matusheski, J. A. Juvik and E. H. Jeffery, Heating decreases epithiospecifier protein activity and increases sulforaphane formation in broccoli, *Phytochemistry*, 2004, **65**, 1273–1281.

17 I. Sarvan, E. Kramer, H. Bouwmeester, M. Dekker and R. Verkerk, Sulforaphane formation and bioaccessibility are more affected by steaming time than meal composition during in vitro digestion of broccoli, *Food Chem.*, 2017, **214**, 580–586.

18 R. Santin-Marquez, A. Alarcon-Aguilar, N. E. Lopez-Diazguerrero, N. Chondrogianni and M. Konigsberg,

Sulforaphane - role in aging and neurodegeneration, *GeroScience*, 2019, **41**, 655–670.

19 V. Zambrano, R. Bustos and A. Mahn, Insights about stabilization of sulforaphane through microencapsulation, *Heliyon*, 2019, **5**, e02951.

20 X. Li, Y. Wang, G. Zhao, G. Liu, P. Wang and J. Li, Microorganisms-An Effective Tool to Intensify the Utilization of Sulforaphane, *Foods*, 2022, **11**, 3775.

21 A. Y. Abuhelwa, D. B. Williams, R. N. Upton and D. J. Foster, Food, gastrointestinal pH, and models of oral drug absorption, *Eur. J. Pharm. Biopharm.*, 2017, **112**, 234–248.

22 J. Grgic, G. Selo, M. Planinic, M. Tisma and A. Bucic-Kojic, Role of the Encapsulation in Bioavailability of Phenolic Compounds, *Antioxidants*, 2020, **9**, 923.

23 M. Mohammadian, M. I. Waly, M. Moghadam, Z. Emam-Djomeh, M. Salami and A. A. Moosavi-Movahedi, Nanostructured food proteins as efficient systems for the encapsulation of bioactive compounds, *Food Sci. Hum. Wellness*, 2020, **9**, 199–213.

24 M. Fathi, F. Donsi and D. J. McClements, Protein-Based Delivery Systems for the Nanoencapsulation of Food Ingredients, *Compr. Rev. Food Sci. Food Saf.*, 2018, **17**, 920–936.

25 B. Zhang, L. Zheng, S. Liang, Y. Lu, J. Zheng, G. Zhang, W. Li and H. Jiang, Encapsulation of Capsaicin in Whey Protein and OSA-Modified Starch Using Spray-Drying: Physicochemical Properties and Its Stability, *Foods*, 2022, **11**, 612.

26 S. Solghi, Z. Emam-Djomeh, M. Fathi and F. Farahani, The encapsulation of curcumin by whey protein: Assessment of the stability and bioactivity, *J. Food Process Eng.*, 2020, **43**, e13403.

27 Y. Hu, G. Kou, Q. Chen, Y. Li and Z. Zhou, Protection and delivery of mandarin (Citrus reticulata Blanco) peel extracts by encapsulation of whey protein concentrate nanoparticles, *LWT – Food Sci. Technol.*, 2019, **99**, 24–33.

28 A. López-Rubio and J. M. Lagaron, Whey protein capsules obtained through electrospraying for the encapsulation of bioactives, *Innovative Food Sci. Emerging Technol.*, 2012, **13**, 200–206.

29 N. Shakoury, M. A. Aliyari, M. Salami, Z. Emam-Djomeh, B. Vardhanabhuti and A. A. Moosavi-Movahedi, Encapsulation of propolis extract in whey protein nanoparticles, *LWT – Food Sci. Technol.*, 2022, **158**, 113138.

30 A. Can Karaca, N. H. Low and M. T. Nickerson, Potential use of plant proteins in the microencapsulation of lipophilic materials in foods, *Trends Food Sci. Technol.*, 2015, **42**, 5–12.

31 M. Henchion, M. Hayes, A. M. Mullen, M. Fenelon and B. Tiwari, Future Protein Supply and Demand: Strategies and Factors Influencing a Sustainable Equilibrium, *Foods*, 2017, **6**, 53.

32 A. Gomes and P. Sobral, Plant Protein-Based Delivery Systems: An Emerging Approach for Increasing the Efficacy of Lipophilic Bioactive Compounds, *Molecules*, 2021, **27**, 60.

33 A. Nesterenko, I. Alric, F. Silvestre and V. Durrieu, Vegetable proteins in microencapsulation: A review of recent interventions and their effectiveness, *Ind. Crops Prod.*, 2013, **42**, 469–479.

34 Q. Guo, X. Shu, Y. Hu, J. Su, S. Chen, E. A. Decker and Y. Gao, Formulated protein-polysaccharide-surfactant ternary complexes for co-encapsulation of curcumin and resveratrol: Characterization, stability and in vitro digestibility, *Food Hydrocolloids*, 2021, **111**, 106265.

35 J. Yi, C. Gan, Z. Wen, Y. Fan and X. Wu, Development of pea protein and high methoxyl pectin colloidal particles stabilized high internal phase pickering emulsions for β-carotene protection and delivery, *Food Hydrocolloids*, 2021, **113**, 106497.

36 F. González, J. Quintero, R. Del Río and A. Mahn, Optimization of an Extraction Process to Obtain a Food-Grade Sulforaphane-Rich Extract from Broccoli (*Brassica oleracea* var. *italica*), *Molecules*, 2021, **26**, 4042.

37 C. Perez, H. Barrientos, J. Roman and A. Mahn, Optimization of a blanching step to maximize sulforaphane synthesis in broccoli florets, *Food Chem.*, 2014, **145**, 264–271.

38 J. S. Garcia-Saldana, O. N. Campas-Baypoli, J. Lopez-Cervantes, D. I. Sanchez-Machado, E. U. Cantu-Soto and R. Rodriguez-Ramirez, Microencapsulation of sulforaphane from broccoli seed extracts by gelatin/gum arabic and gelatin/pectin complexes, *Food Chem.*, 2016, **201**, 94–100.

39 A. Ali Redha, H. T. Hong, L. Torquati, G. R. Nash, M. J. Gidley and D. Cozzolino, Development of Liquid Chromatography-Mass Spectrometry (LC-MS) Method for Quantification of Broccoli Sulforaphane, *Food Anal. Methods*, 2024, **17**, 1–6.

40 K. Molly, M. V. Woestyne, I. D. Smet and W. Verstraete, Validation of the Simulator of the Human Intestinal Microbial Ecosystem (SHIME) Reactor Using Microorganism-associated Activities, *Microb. Ecol. Health Dis.*, 1994, **7**, 191–200.

41 D. P. Baptista, M. K. Salgaço, K. Sivieri and M. L. Gigante, Use of static and dynamic in vitro models to simulate Prato cheese gastrointestinal digestion: Effect of Lactobacillus helveticus LH-B02 addition on peptides bioaccessibility, *LWT – Food Sci. Technol.*, 2020, **134**, 110229.

42 M. Minekus, M. Alminger, P. Alvito, S. Ballance, T. Bohn, C. Bourlieu, F. Carriere, R. Boutrou, M. Corredig, D. Dupont, C. Dufour, L. Egger, M. Golding, S. Karakaya, B. Kirkhus, S. Le Feunteun, U. Lesmes, A. Macierzanka, A. Mackie, S. Marze, D. J. McClements, O. Menard, I. Recio, C. N. Santos, R. P. Singh, G. E. Vegarud, M. S. Wickham, W. Weitschies and A. Brodkorb, A standardised static in vitro digestion method suitable for food - an international consensus, *Food Funct.*, 2014, **5**, 1113–1124.

43 S. Akter, R. Addepalli, M. Netzel, U. Tinggi, M. Fletcher, Y. Sultanbawa and S. Osborne, In vitro Bioaccessibility and

Intestinal Absorption of Selected Bioactive Compounds in Terminalia ferdinandiana, *Front. Nutr.*, 2021, **8**, 818195.

44 J. B. Foo, L. S. Ng, J. H. Lim, P. X. Tan, Y. Z. Lor, J. S. E. Loo, M. L. Low, L. C. Chan, C. Y. Beh, S. W. Leong, L. Saiful Yazan, Y. S. Tor and C. W. How, Induction of cell cycle arrest and apoptosis by copper complex Cu(SBCM)(2) towards oestrogen-receptor positive MCF-7 breast cancer cells, *RSC Adv.*, 2019, **9**, 18359–18370.

45 W. Zhu, L. A. Lerno, E. Cremonini, P. I. Oteiza, A. Mastaloudis, G. M. Bornhorst and A. E. Mitchell, Robust UHPLC-(ESI+)-MS/MS Method for Simultaneous Analysis of Glucoraphanin, Sulforaphane, and Sulforaphane Metabolites in Biological Samples, *ACS Food Sci. Technol.*, 2023, **3**, 1300–1310.

46 E. S. Hwang, G. M. Bornhorst, P. I. Oteiza and A. E. Mitchell, Assessing the Fate and Bioavailability of Glucosinolates in Kale (Brassica oleracea) Using Simulated Human Digestion and Caco-2 Cell Uptake Models, *J. Agric. Food Chem.*, 2019, **67**, 9492–9500.

47 I. Hubatsch, E. G. Ragnarsson and P. Artursson, Determination of drug permeability and prediction of drug absorption in Caco-2 monolayers, *Nat. Protoc.*, 2007, **2**, 2111–2119.

48 M. Barati, F. Javanmardi, S. M. H. Mousavi Jazayeri, M. Jabbari, J. Rahmani, F. Barati, H. Nickho, S. H. Davoodi, N. Roshanravan and A. Mousavi Khaneghah, Techniques, perspectives, and challenges of bioactive peptide generation: A comprehensive systematic review, *Compr. Rev. Food Sci. Food Saf.*, 2020, **19**, 1488–1520.

49 W. Yuanfeng, L. Chengzhi, Z. Ligen, S. Juan, S. Xinjie, Z. Yao and M. Jianwei, Approaches for enhancing the stability and formation of sulforaphane, *Food Chem.*, 2021, **345**, 128771.

50 Z. Azarashkan, A. Motamedzadegan, A. Ghorbani-HasanSaraei, S. Rahaiee and P. Biparva, Improvement of the Stability and Release of Sulforaphane-enriched Broccoli Sprout Extract Nanoliposomes by Co-encapsulation into Basil Seed Gum, *Food Bioprocess Technol.*, 2022, **15**, 1573–1587.

51 P. Garcia-Ibanez, D. A. Moreno and M. Carvajal, Nanoencapsulation of Bimi(R) extracts increases its bioaccessibility after in vitro digestion and evaluation of its activity in hepatocyte metabolism, *Food Chem.*, 2022, **385**, 132680.

52 G. B. Martinez-Hernandez, T. Venzke-Klug, M. D. M. Carrion-Monteagudo, F. Artes Calero, J. M. Lopez-Nicolas and F. Artes-Hernandez, Effects of alpha-, beta- and maltosyl-beta-cyclodextrins use on the glucoraphanin-sulforaphane system of broccoli juice, *J. Sci. Food Agric.*, 2019, **99**, 941–946.

53 P. Abassi, F. Abassi, F. Yari, M. Hashemi and S. Nafisi, Study on the interaction of sulforaphane with human and bovine serum albumins, *J. Photochem. Photobiol., B*, 2013, **122**, 61–67.

54 K. Youn, J. H. Yoon, N. Lee, G. Lim, J. Lee, S. Sang, C. T. Ho and M. Jun, Discovery of Sulforaphane as a Potent BACE1 Inhibitor Based on Kinetics and Computational Studies, *Nutrients*, 2020, **12**, 3026.

55 M. F. Alam, A. A. Laskar, L. Maryam and H. Younus, Activation of Human Salivary Aldehyde Dehydrogenase by Sulforaphane: Mechanism and Significance, *PLoS One*, 2016, **11**, e0168463.

56 A. C. Yue, X. D. Zhou, H. P. Song, X. H. Liu, M. J. Bi, W. Han and Q. Li, Effect and molecular mechanism of Sulforaphane alleviates brain damage caused by acute carbon monoxide poisoning:Network pharmacology analysis, molecular docking, and experimental evidence, *Environ. Toxicol.*, 2024, **39**, 1140–1162.

57 Y. Rezende, J. P. Nogueira and N. Narain, Microencapsulation of extracts of bioactive compounds obtained from acerola (Malpighia emarginata DC) pulp and residue by spray and freeze drying: Chemical, morphological and chemometric characterization, *Food Chem.*, 2018, **254**, 281–291.

58 C. Yamashita, M. M. S. Chung, C. dos Santos, C. R. M. Mayer, I. C. F. Moraes and I. G. Branco, Microencapsulation of an anthocyanin-rich blackberry (Rubus spp.) by-product extract by freeze-drying, *LWT – Food Sci. Technol.*, 2017, **84**, 256–262.

59 M. E. da Silva Junior, M. Araujo, A. C. S. Martins, M. Dos Santos Lima, F. L. H. da Silva, A. Converti and M. I. S. Maciel, Microencapsulation by spray-drying and freeze-drying of extract of phenolic compounds obtained from ciriguela peel, *Sci. Rep.*, 2023, **13**, 15222.

60 S. Tatasciore, V. Santarelli, L. Neri, R. Gonzalez Ortega, M. Faieta, C. D. Di Mattia, A. Di Michele and P. Pittia, Freeze-Drying Microencapsulation of Hop Extract: Effect of Carrier Composition on Physical, Techno-Functional, and Stability Properties, *Antioxidants*, 2023, **12**, 442.

61 P. N. Ezhilarasi, D. Indrani, B. S. Jena and C. Anandharamakrishnan, Freeze drying technique for microencapsulation of Garcinia fruit extract and its effect on bread quality, *J. Food Eng.*, 2013, **117**, 513–520.

62 A. Rezvankhah, Z. Emam-Djomeh and G. Askari, Encapsulation and delivery of bioactive compounds using spray and freeze-drying techniques: A review, *Drying Technol.*, 2019, **38**, 235–258.

63 J. Andrade, C. G. Pereira, J. C. d. Almeida Junior, C. C. R. Viana, L. N. d. O. Neves, P. H. F. d. Silva, M. J. V. Bell and V. d. C. d. Anjos, FTIR-ATR determination of protein content to evaluate whey protein concentrate adulteration, *LWT – Food Sci. Technol.*, 2019, **99**, 166–172.

64 G. R. De Nicola, P. Rollin, E. Mazzon and R. Iori, Novel gram-scale production of enantiopure R-sulforaphane from Tuscan black kale seeds, *Molecules*, 2014, **19**, 6975–6986.

65 P. K. Revelou, M. G. Kokotou, C. S. Pappas and V. Constantinou-Kokotou, Direct determination of total isothiocyanate content in broccoli using attenuated total reflectance infrared Fourier transform spectroscopy, *J. Food Compos. Anal.*, 2017, **61**, 47–51.

66 J. K. Ahmed, Z. J. Abdul Amer and M. J. M. Al-Bahate, Effect of chlorophyll and anthocyanin on the secondary

bonds of polymethyl methacrylate (PMMA), *Int. J. Tech. Res. Appl.*, 2014, **2**, 73–80.

67 A. Ali Redha, L. Torquati, F. Langston, G. R. Nash, M. J. Gidley and D. Cozzolino, Determination of glucosinolates and isothiocyanates in glucosinolate-rich vegetables and oilseeds using infrared spectroscopy: A systematic review, *Crit. Rev. Food Sci. Nutr.*, 2024, **64**, 8248–8264.

68 G. K. Gbassi, F. S. Yolou, S. O. Sarr, P. G. Atheba, C. N. Amin and M. Ake, Whey proteins analysis in aqueous medium and in artificial gastric and intestinal fluids, *Int J. Biol. Chem. Sci.*, 2012, **6**, 1828–1837.

69 S. Saah, D. Siriwan, P. Trisonthi and S. Dueramae, Physicochemical and biological properties of encapsulated Boesenbergia rotunda extract with different wall materials in enhancing antioxidant, mineralogenic and osteogenic activities of MC3T3-E1 cells, *Saudi Pharm. J.*, 2024, **32**, 101998.

70 Q. Shekarri and M. Dekker, A Physiological-Based Model for Simulating the Bioavailability and Kinetics of Sulforaphane from Broccoli Products, *Foods*, 2021, **10**, 2761.

71 A. Abellan, R. Dominguez-Perles, C. Garcia-Viguera and D. A. Moreno, Evidence on the Bioaccessibility of Glucosinolates and Breakdown Products of Cruciferous Sprouts by Simulated In Vitro Gastrointestinal Digestion, *Int. J. Mol. Sci.*, 2021, **22**, 11046.

72 E. C. Thuenemann, in *The Impact of Food Bioactives on Health - in vitro and ex vivo models*, ed. K. Verhoeckx, P. Cotter, I. López-Expósito, C. Kleiveland, T. Lea, A. Mackie, T. Requena, D. Swiatecka and H. Wichers, Springer, 2015.

73 D. Dupont, M. Alric, S. Blanquet-Diot, G. Bornhorst, C. Cueva, A. Deglaire, S. Denis, M. Ferrua, R. Havenaar, J. Lelieveld, A. R. Mackie, M. Marzorati, O. Menard, M. Minekus, B. Miralles, I. Recio and P. Van den Abbeele, Can dynamic in vitro digestion systems mimic the physiological reality?, *Crit. Rev. Food Sci. Nutr.*, 2019, **59**, 1546–1562.

74 A. R. Madureira, C. I. Pereira, A. M. P. Gomes, M. E. Pintado and F. Xavier Malcata, Bovine whey proteins – Overview on their main biological properties, *Food Res. Int.*, 2007, **40**, 1197–1211.

75 S. H. M. Gorissen, J. J. R. Crombag, J. M. G. Senden, W. A. H. Waterval, J. Bierau, L. B. Verdijk and L. J. C. van Loon, Protein content and amino acid composition of commercially available plant-based protein isolates, *Amino Acids*, 2018, **50**, 1685–1695.

76 H. Husband, S. Ferreira, F. Bu, S. Feyzi and B. P. Ismail, Pea protein globulins: Does their relative ratio matter?, *Food Hydrocolloids*, 2024, **148**, 109429.

77 G. S. Silva, M. H. G. Gomes, L. M. de Carvalho, T. L. Abreu, M. Dos Santos Lima, M. S. Madruga, L. E. Kurozawa and T. K. A. Bezerra, Microencapsulation of organic coffee husk polyphenols: Effects on release, bioaccessibility, and antioxidant capacity of phenolics in a simulated gastrointestinal tract, *Food Chem.*, 2024, **434**, 137435.

78 A. Akbarzadeh, R. Rezaei-Sadabady, S. Davaran, S. W. Joo, N. Zarghami, Y. S. Hanifehpour, S. Mohammad, M. Kouhi and K. Nejati-Koshki, Liposome: classification, preparation, and applications, *Nanoscale Res. Lett.*, 2013, **8**, 102.

79 L. B. Olvera-Rosales, A. E. Cruz-Guerrero, J. M. Garcia-Garibay, L. C. Gomez-Ruiz, E. Contreras-Lopez, F. Guzman-Rodriguez and L. G. Gonzalez-Olivares, Bioactive peptides of whey: obtaining, activity, mechanism of action, and further applications, *Crit. Rev. Food Sci. Nutr.*, 2023, **63**, 10351–10381.

80 N. P. K. Le, M. J. Altenburger and E. Lamy, Development of an Inflammation-Triggered In Vitro "Leaky Gut" Model Using Caco-2/HT29-MTX-E12 Combined with Macrophage-like THP-1 Cells or Primary Human-Derived Macrophages, *Int. J. Mol. Sci.*, 2023, **24**, 7427.

81 C. R. Kleiveland, in *The Impact of Food Bioactives on Health: in vitro and ex vivo models*, ed. K. Verhoeckx, P. Cotter, I. López-Expósito, C. Kleiveland, T. Lea, A. Mackie, T. Requena, D. Swiatecka and H. Wichers, Springer, 2015.

82 I. Lozoya-Agullo, F. Araujo, I. Gonzalez-Alvarez, M. Merino-Sanjuan, M. Gonzalez-Alvarez, M. Bermejo and B. Sarmento, Usefulness of Caco-2/HT29-MTX and Caco-2/HT29-MTX/Raji B Coculture Models To Predict Intestinal and Colonic Permeability Compared to Caco-2 Monoculture, *Mol. Pharm.*, 2017, **14**, 1264–1270.

83 C. Dima, E. Assadpour, S. Dima and S. M. Jafari, Bioavailability of nutraceuticals: Role of the food matrix, processing conditions, the gastrointestinal tract, and nanodelivery systems, *Compr. Rev. Food Sci. Food Saf.*, 2020, **19**, 954–994.

84 N. Petri, C. Tannergren, B. Holst, F. A. Mellon, Y. Bao, G. W. Plumb, J. Bacon, K. A. O'leary, P. A. Kroon, L. Knutson, P. Forsell, T. Eriksson, H. Lennernas and G. Williamson, Absorption/metabolism of sulforaphane and quercetin, and regulation of phase ii enzymes, in human jejunum in vivo, *Drug Metab. Dispos.*, 2003, **31**, 805–813.

85 S. Winiwarter, N. M. Bonham, F. Ax, A. Hallberg, H. Lennernäs and A. Karlén, Correlation of Human Jejunal Permeability (in Vivo) of Drugs with Experimentally and Theoretically Derived Parameters. A Multivariate Data Analysis Approach, *J. Med. Chem.*, 1998, **41**, 4939–4949.

86 A. Tarozzi, C. Angeloni, M. Malaguti, F. Morroni, S. Hrelia and P. Hrelia, Sulforaphane as a potential protective phytochemical against neurodegenerative diseases, *Oxid. Med. Cell. Longevity*, 2013, **2013**, 415078.

87 A. V. Gasper, A. Al-janobi, J. A. Smith, J. R. Bacon, P. Fortun, C. Atherton, M. A. Taylor, C. J. Hawkey, D. A. Barrett and R. F. Mithen, Glutathione S-transferase M1 polymorphism and metabolism of sulforaphane from standard and high-glucosinolate broccoli, *Am. J. Clin. Nutr.*, 2005, **82**, 1283–1291.

88 M. Traka, A. V. Gasper, A. Melchini, J. R. Bacon, P. W. Needs, V. Frost, A. Chantry, A. M. Jones, C. A. Ortori, D. A. Barrett, R. Y. Ball, R. D. Mills and R. F. Mithen,

Broccoli consumption interacts with GSTM1 to perturb oncogenic signalling pathways in the prostate, *PLoS One*, 2008, **3**, e2568.

89 S. Biswas and I. Rahman, in *Bioactive Food as Dietary Interventions for Liver and Gastrointestinal Disease*, ed. R. R. Watson and V. R. Preedy, Academic Press, 2013, pp. 513–525.

90 A. A. Al Janobi, R. F. Mithen, A. V. Gasper, P. N. Shaw, R. J. Middleton, C. A. Ortori and D. A. Barrett, Quantitative measurement of sulforaphane, iberin and their mercapturic acid pathway metabolites in human plasma and urine using liquid chromatography-tandem electrospray ionisation mass spectrometry, *J. Chromatogr. B: Anal. Technol. Biomed. Life Sci.*, 2006, **844**, 223–234.